

EPSC2018  
**SB3 abstracts**

## Access to Phobos data at updated version of MExLab Planetary data Geoportal

A.S. Garov, I.P. Karachevtseva, A.E. Zubarev, I.E. Nadezhkina, N.A. Kozlova  
Moscow State University of Geodesy and Cartography (MIIGAiK), MIIGAiK Extraterrestrial Laboratory (MExLab),  
Moscow, Russia (i\_karachevtseva@miiigaik.ru)

### Abstract

To store results of planetary image processing and spatial surface analysis we are creating a Geoportal of Planetary Data. The first pilot version of information system as 2D web GIS (<http://cartsrv.mexlab.ru/geoportal/>) was based on Phobos data processed in frame of preparation for Phobos-Grunt mission [1].

New Geoportal will allow full and effective exploitation of data for planetary research with web access and interactive online tools for high-level analysis of planetary data. The web-platform organized as an online 3D web-GIS portal. The web-portal and applications have a unified basic interface, implemented using HTML markup. Based on the new software architecture [2], several cross-platform solutions are developed to integrate various collections of planetary data. Some executable applications that have been created using new software architecture and developed infrastructure will be presented at the conference.

### References

- [1] Nadezhkina I., Zubarev A., Patraty V., Shishkina L., Zharov O., Zharov A., Oberst J. Phobos Control Point Network and Librations. // European Planetary Science Congress, September 23-28, 2012, Madrid, Spain, [EPSC2012-238].  
[http://www.epsc2012.eu/epsc2012\\_session\\_overview.pdf](http://www.epsc2012.eu/epsc2012_session_overview.pdf).
- [2] Garov A.S., Karachevtseva I.P., Matveev E.V., Zubarev A.E., Patraty V.D. (2016) Development of heterogenic distributed environment for spatial data processing using cloud technologies. 2016. The International Archives of the Photogrammetry, Remote Sensing and Spatial Information Sciences, Vol. XLI-B4, pp. 385-390, XXIII ISPRS Congress, 12–19 July 2016, Prague. doi:10.5194/isprs-archives-XLI-B4-385-2016/.

## Spectral modeling (0.5-2.5 $\mu\text{m}$ ) of the Phobos Blue-Red transition area

**Maurizio Pajola** (1), Ted Roush (2), Cristina Dalle Ore (2,3), Giuseppe A. Marzo (4) and Emanuele Simioni (1)  
(1) INAF, Osservatorio Astronomico di Padova, Vicolo dell'Osservatorio 5, 35122, Padova, Italy (maurizio.pajola@oapd.inaf.it), (2) NASA Ames Research Center, Moffett Field, CA, 94035, USA, (3) Carl Sagan Center, SETI Institute, Mountain View, CA, 94043, USA, (4) ENEA C. R. Casaccia, 00123, Roma, Italy

### Abstract

We here focus on the spectral modeling of the surface of Phobos in the wavelength range between 0.5 and 2.5  $\mu\text{m}$  exploiting the Phobos Mars Reconnaissance Orbiter/Compact Reconnaissance Imaging Spectrometer for Mars (MRO/CRISM) dataset obtained on 2007 October 23. The spatial scale of this dataset is 355 m/pixel, while the phase angle of the observation is  $\sim 37.5^\circ$  [1]. The CRISM observation covers the sub-Mars hemisphere of Phobos, from Stickney crater's interior and rim, to the limit between the leading and trailing hemispheres of the satellite (Fig. 1A). This area is of particular interest because it is the most variegated region on Phobos and it has different spectral slopes in the Vis/NIR wavelength range. The fresher areas close to Stickney crater have a lower color ratio, and are the "Blue unit" of [2], Fig. 1B. This unit is considered as the fresh ejecta deposit excavated from the interior of Phobos and resulting from the oblique impact that generated Stickney. Instead, the background areas are characterized by a higher ratio and are the "Red unit" of [3].

Without a priori selecting specific surface locations, we include spectra from nearly the entire surface observed. We use the unsupervised K-means partitioning algorithm developed by [4] in order to investigate the spectral variability across Phobos' surface. This technique has been extensively validated using spectral data sets and applied to Mars [4-6], Iapetus [7,8], Charon [9] and Mercury [10]. After correcting the CRISM data to a standard viewing geometry (using incidence and emission maps to minimize the influence of local topography on the spectra), the statistical partitioning identifies seven clusters over the observed surface of Phobos (Fig. 1C). From these clusters we eliminate both cluster 0, that corresponds to the space around Phobos and those associated to the limb/terminator of

the satellite (clusters no. 1 and 2), and then investigate the compositional information contained within the average spectra of the remaining four clusters by using the radiative transfer model of [11].

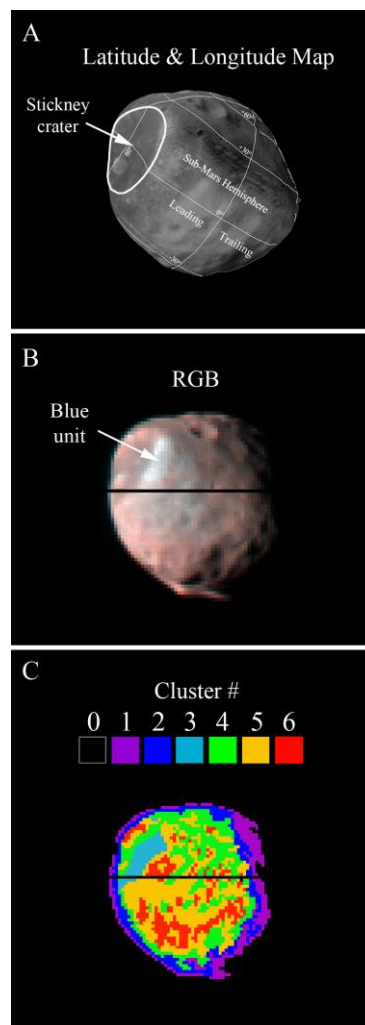


Fig. 1: A) The Phobos area observed by CRISM. B) RGB image from CRISM Vis region (R=0.90  $\mu\text{m}$ , G=0.58  $\mu\text{m}$ , B=0.50  $\mu\text{m}$ ). C) The seven clusters identified on Phobos.

As previously suggested by [12], we use the optical constants of Tagish Lake meteorite (TL, [13]), and pyroxene glass (PM80, [14,15]) as inputs for the calculations. The results show a good slope agreement when compared to the averages of the CRISM spectral clusters (Fig. 2). In particular, the best fitting model of the cluster with the steepest spectral slope (cluster no. 6) yields relative abundances that are equal to those of [12], i.e. 20% PM80 and 80% TL, but grain sizes that are slightly different with respect to [12].

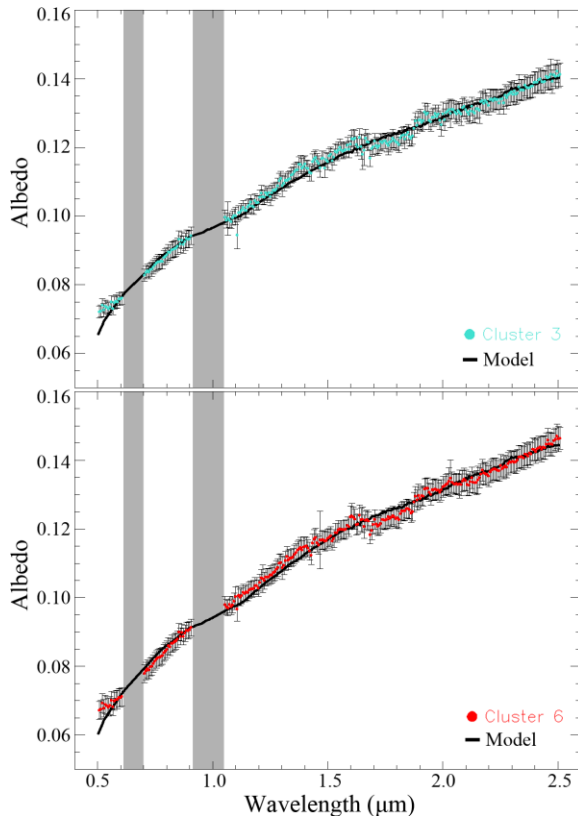


Fig. 2: The spectra of clusters 3 and 6 with the corresponding models. The bars associated correspond to the  $1\sigma$  values. The grey bars indicate the CRISM bad bands not considered in the modeling.

Such discrepancy may arise from the fact that the areas observed in this work and those analyzed in [12] are on opposite locations on Phobos and present different morphological and weathering settings. On the contrary, as the clusters spectral slopes decrease, the best fits obtained show trends related to both relative abundance and grain size that is not observed for the cluster with the steepest spectral slope. With a decrease in slope there is general increase of relative percentage of PM80 from 12% to 18% and the

associated decrease of TL from 88% to 82%. Simultaneously the PM80 grain sizes decrease from 9 to 5  $\mu\text{m}$  and TL grain sizes increase from 13 to 16  $\mu\text{m}$ .

The best fitting models show relative abundances and grain sizes that partially overlap. This supports the hypothesis that from a compositional perspective the transition between the highest and lowest slopes on Phobos is subtle, and it is characterized by a smooth change of relative abundances and grain sizes, rather than a distinct dichotomy between the areas.

## Acknowledgements

M.P. was supported for this research by an appointment to the NASA Postdoctoral Program at the Ames Research Center, administered by Universities Space Research Association (USRA) through a contract with NASA. The NASA PDS Archive node is acknowledged for providing access to the CRISM dataset used in this work.

## References

- [1] Pajola, M. et al., 2018. *Planet. Space Sci.* 154, 63-71.
- [2] Murchie, S., Erard, S., 1996. *Icarus* 123, 63.
- [3] Murchie, S., et al., 1999. *J. Geophys. Res.* 104, 9069–9080.
- [4] Marzo, G., et al., 2006. *J. Geophys. Res.* 111. E03002.
- [5] Marzo, G., et al., 2008. *J. Geophys. Res.* 113. E12009.
- [6] Fonti, S., Marzo, G.A., 2010. *Astron. Astrophys.* 512 (A51), 6 pp.
- [7] Pinilla-Alonso, N., et al., 2011. *Icarus* 215 (1), 75.
- [8] Dalle Ore, C., et al., 2012. *Icarus* 221 (2), 735.
- [9] Dalle Ore, C., et al., 2018. *Icarus* 300, 21–32.
- [10] Lucchetti, et al., 2017. *48 Lunar and Planetary Science Conference*, 1964.
- [11] Shkuratov, Y., et al., 1999. *Icarus* 137, 235.
- [12] Pajola, M., et al., 2013. *Astrophys. J.* 777, 127, 6 pp.
- [13] Roush, T.L., 2003. *M&PS* 38, 419.
- [14] Jaeger, C., et al. 1994. *Astron. Astrophys.* 292, p. 641.
- [15] Dorschner, J., et al. 1995. *Astron. Astrophys.* 300, p. 503.

# Simulations of Impact Gardening on Phobos

**Dana Hurley**

Johns Hopkins Applied Physics Laboratory, Laurel, MD, USA (dana.hurley@jhuapl.edu)

## Abstract

The continual bombardment of Solar System bodies by meteoroids contributes to the creation and mixing of regolith. This paper investigates the impact gardening process on Mars' moon Phobos. The investigation focuses on the effects of impacts on the formation of topographical features on Phobos. Further, it calculates the formation of regolith and how the properties of regolith depend on the impact crater morphology used. The factor with largest influence on the model output is the fraction of ejecta that is emplaced in a blanket vs. launched into orbit around Mars. The thickness of the regolith is a method to distinguish between those ejecta blanket emplacement scenarios.

## 1. Introduction

Whether Phobos is an asteroid that was captured into Mars' orbit or if it formed in Mars' orbit is an important question. The upcoming JAXA MMX mission will study Phobos through remote sensing, then return a sample. It is well-known that surfaces of bodies exposed to space are subjected to multiple processes that "weather" the surface. One process called impact gardening creates regolith and mixes it with depth. Impact gardening has a significant effect on the surface of a body; and therefore, it must be considered when interpreting remote sensing data and samples originating on the surface. In this paper, I simulate the effects of impact gardening on the overturn of regolith for Phobos including the lateral transport of material and the time evolution of topography.

## 2. Model Description

A Monte Carlo technique adapted from lunar simulations to simulate the stochastic process of impact gardening [1-4] is applied to the surface of Phobos. The model uses the crater production function as a basis

for generating impact craters over time [5-6]. The model explicitly follows the topography in a patch of surface of area 20 m x 20 m. However, impacts are generated over a larger area as some impacts centered outside of the box still contribute to the interior of the box. Thus the impact generation box is larger than the simulation box. The model implements impacts by calculating a bowl shape crater of the size and coordinates determined by the program. The code alters the topography within the crater by replacing the existing topography with the new bowl at an altitude centered on the previous average altitude of the area. An ejecta blanket is deposited with a distance-dependent thickness overlying the pre-existing topography outside of the rim. The program iterates through this process for the duration of the simulated time window.

The code simply tracks the current topography of the surface and the minimum topography. This combination of values provides much information about the generation of regolith and features on Phobos.

By conducting multiple runs with the same initial conditions and a different seed to the random number generator, the model calculates the probability of situations occurring. This technique will never be able to reproduce the exact impact history of a particular area. However, by repeating the simulations with varied initial conditions, we calculate the dependence of the expectation values on the inputs.

## 3. Results

Using nominal crater morphology, the mean altitude of the surface of Phobos slowly inflates with time. This results from the ratio of the volume of the ejecta to the volume of the excavated crater. Mass is conserved, however the density in the ejecta blanket is lower than that of the bedrock.

In addition, the thickness of the regolith and the roughness of the surface are computed. If Phobos contains phyllosilicates or other native volatiles, the calculation provides the depth where impacts have not affected the contents. In contrast, if exogenous volatiles from Mars or meteoroids are delivered to Mars, the regolith layer is the place where they would be deposited.

However, these values are dependent of the choice of crater morphology. The ratio of excavated volume to ejecta volume may change depending on the amount of escape that is expected for the ejecta. Likewise, the lateral extent of the ejecta blanket will influence the roughness and the variability in regolith thickness. The model demonstrates how the regolith thickness, once measured at Phobos, can provide constraints on the crater ejecta escape rate.

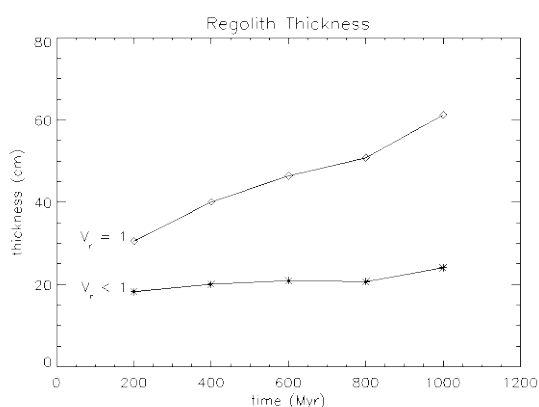


Figure 1: The time evolution of regolith thickness on Phobos is shown for two different assumptions about the escape of impact ejecta. For nominal conditions, the thickness of regolith increases over time reaching 60 cm in 1 Gyr.

## 4. Summary and Conclusions

The results of the impact gardening model can be used in understanding the time history of the surface of Mars' Moon Phobos in relation to remote sensing measurements from MMX or potential cubesat missions to Phobos.

## Acknowledgements

Funding for this work was provided by NASA SSERVI and NASA PSDS3.

## References

- [1] Arnold J. R. (1975) LSC VI, 2375-2395.
- [2] Borg J. et al. (1976) EPSL, 29, 161-174.
- [3] Crider D. H. and Vondrak R. R. (2003) JGR, 108, 5079.
- [4] Hurley D. M. et al. (2012) Geophys. Rev. Lett., 39, L09203.
- [5] Schmedemann N. et al. (2014) Planet. Sp. Sci., 102, 152-163.
- [6] Christou A. A. et al. (2014) Planet. Sp. Sci., 102, 164-170.

# Illumination Conditions in Phobos' Polar Areas

Ramona Ziese (1), Konrad Willner (2) and Jürgen Oberst (1,2)

(1) Technische Universität Berlin, Berlin, Germany, (2) German Aerospace Center (DLR), Institute of Planetary Research, Berlin, Germany (ziese@tu-berlin.de)

## Abstract

The illumination conditions in Phobos' polar areas are studied taking into account direct illumination by the Sun, eclipses by Mars and single scattering of solar light by other surface areas of Phobos. Developments to include the contribution of Mars' reflected energy are on the way.

## 1. Introduction

In recent years the Martian moon Phobos was identified as a target by several planetary mission proposals. Precise illumination and thermal models are critical information to plan landed missions and require careful analysis of direct solar irradiation and indirect contributions such as solar light reflected by Mars, thermal emissions from Mars and self-heating of Phobos' surface, i.e. direct thermal radiation emitted from the surrounding surface as well solar light and thermal radiation reflected by the neighborhood.

Phobos moves near the equatorial plane of Mars, with its rotational axis near-perpendicular to its orbit plane, resulting in strong variations of the solar irradiation and thus to seasons, just like on Mars.

This study focuses on the illumination conditions in Phobos' polar areas (above  $+65^\circ$ / below  $-65^\circ$  latitude) which are of interest to future landed missions. Illumination models from this study will also serve as a basis for a subsequent study of the thermal conditions.

## 2. Previous Work

Since detailed shape models were not available at the time, previous investigators [1], [2] used simple ellipsoid models to estimate Phobos' surface temperatures and heat transfer to subsurface layers at discrete surface points.

In addition to solar radiation and the effects of eclipses by Mars, reflected sunlight and thermal radiation from Mars were taken into account, which were

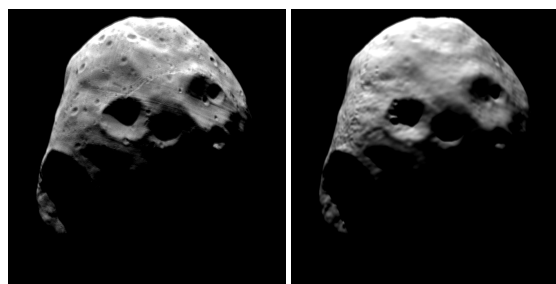


Figure 1: Phobos' Northern hemisphere. Left: SRC image H8870\_0006 (ESA/DLR/FU Berlin (G. Neukum)). Right: Synthetic image.

demonstrated to cause an increased average temperature on the Mars-facing-side of Phobos in its synchronous rotation [1]. In contrast, [3] and [7] studied the direct incident solar flux for Phobos using a recent shape model [5]. Global charts of incident solar flux for certain fixed dates in different seasons [3] as well as average incident solar flux for a complete Martian year [7] were derived.

## 3. Methods

The simulated illumination is based on the ephemerides model NOE-4-2015-b, having the least deviation in comparison to astrometric observations [6], a global shape model of Phobos comprising 274,874 facets [5], and an updated rotational model for Phobos [4]. The illumination of all facets within the North and South pole regions is modeled considering direct illumination by the Sun, eclipses by Mars and single scattering by neighboring surface areas.

To verify the quality of the input models, synthetic images, based on illumination and viewing geometry of original Super Resolution Channel (SRC) images taken by Mars Express were computed. These simulated images show excellent agreement with the originals. An example is provided in Fig. 1.

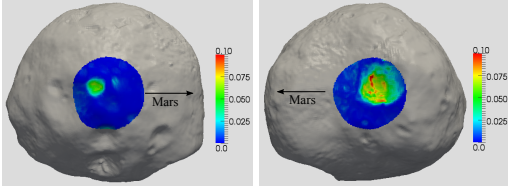


Figure 2: Total view factors for the North (left) and South (right) polar regions.

### 3.1. Direct illumination: Horizon method

For each facet the horizon is pre-computed and stored in a look-up table. At time intervals of currently 10 minutes azimuth and elevation of the Sun are computed and compared with the horizon line. Moreover, the percentage of the visible Sun disk is determined. The advantages of this method are a higher efficiency in the computing, compared to ray-tracing methods and a higher precision on the incoming solar flux rate.

### 3.2. Indirect Illumination: View factors

To include scattering by Phobos' surface onto other parts of Phobos the view factors  $F_{ij}$  indicating the fraction of flux radiated by facet  $j$  that reaches facet  $i$  are computed. Moreover, the total view factors

$$F_i = \sum_j F_{ij} \in [0, 1] \quad (1)$$

were determined. A facet having a total view factor of 0 does not receive any irradiation from other facets while for a facet having a total view factor of 1 the field of view is completely filled by other facets of the surface. Note that we consider single-scattering only.

Fig. 2 shows the total view factors for the North and the South pole region. For the North pole region the maximum total view factor is 0.07, about half of what is found for the more concave-shaped South pole region, where the maximum value is 0.13. In both cases, such secondary irradiation is small when compared to direct insolation, but relevant for facets that are not directly illuminated, and would be in complete darkness without such scattered light.

## 4. Preliminary results and outlook

For both polar regions illumination maps for several time intervals ranging from a few seconds to a Martian year have been computed. During winter seasons, polar areas are in complete darkness, while in the summer, polar areas enjoy longer periods in full sunlight. During spring and fall, illumination is interrupted by

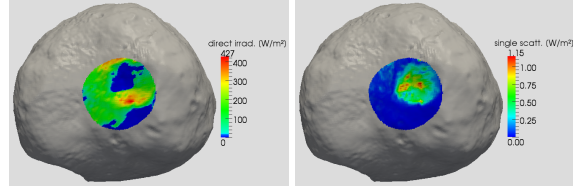


Figure 3: Direct solar irradiation (left) and single scattering (right) off other facets in  $\frac{W}{m^2}$  for the Southern polar region at epoch 2018-06-22T23:10:00 (in Southern spring). Note the different scales of the color codes.

frequent occultations by Mars. Certain areas (in particular South polar) frequently do not receive direct solar irradiation for several hours but are exposed to scattered light only. Fig. 3 exemplarily displays the contributions of direct solar irradiation and single scattering to the total irradiation for the Southern polar region at epoch 2018-06-22T23:10:00. Though these contributions are small, they might be relevant for future thermal modeling. The contribution of Mars-reflected solar light and thermal emissions by Mars' surface is currently considered and computed. Preliminary results will be reported at the meeting.

## Acknowledgements

This project is supported by the Deutsche Forschungsgemeinschaft (DFG), research grant number OB 124/14-1. The authors thank the HRSC Experiment teams for their successful planning and acquisition of data as well as for making processed data available to the HRSC team.

## References

- [1] Kührt, E. and Giese, B.: A thermal model of the Martian satellites, Icarus, 81, pp. 102-112, 1989.
- [2] Kuzmin R. O., Zabalueva, E. V.: The Temperature Regime of the Surface Layer of the Phobos Regolith in the Region of the Potential Fobos-Grunt Space Station Landing Site, Solar System Res. 37, pp. 480-488, 2003.
- [3] Li, Z. Q. et al.: Lighting condition analysis for Mars' Moon Phobos, 2016 IEEE Aerospace Conference, 5-12 March 2016, Big Sky (MT), USA, 2016.
- [4] Stark, A. et. al.: Geodetic Framework for Martian Satellite Exploration I, European Planetary Science Congress 2017, 17-22 September 2017, Riga, Latvia.
- [5] Willner, K.: Phobos' shape and topography models, PSS, 102, pp. 51-59, 2014.
- [6] Ziese, R. and Willner, K.: Mutual event observations of solar system objects by SRC on Mars Express, A&A, in press, 2018.
- [7] Stubbs, T. J. et. al.: Illumination Conditions on Phobos: Implications for Surface Processes, Volatiles, and Exploration, Lunar and Planetary Science Conference, 20-24 March 2017, The Woodlands, Texas, 2017.

# Mutual Event Observations of the Martian moons by SRC on Mars Express

Konrad Willner (1), Ramona Ziese (2), and Jürgen Oberst (1,2)

(1) German Aerospace Center (DLR), Institute of Planetary Research, Berlin, Germany, (konrad.willner@dlr.de)

(2) Technische Universität Berlin, Berlin, Germany, (ziese@tu-berlin.de)

## Abstract

The positions of the Martian moons are determined in so-called "mutual event" images acquired by the Super Resolution Channel (SRC) of the High Resolution Stereo Camera aboard Mars Express. These images depict either of the moons *and* the Earth-Moon system, the Galilean moons, the Martian surface, a star or a star field. Such mutual event observations are obtained on a regular basis with the SRC and support the determination of ephemerides for the two satellites.

## 1. Introduction

Astrometric observations are critical for studies of positions or orbits of planets and satellites. Past SRC astrometric observations containing Phobos or Deimos alone require accurate spacecraft pointing information or means to consider pointing offsets or random errors [5, 6, 7, 11].

Recently, we focused on mutual event observations containing objects filling several pixels in the image, e.g. both moons or either Jupiter or Saturn in the background, and determined the relative angular separation between the imaged bodies. For these kinds of observations the pointing of the spacecraft is irrelevant [13]. Here, we report on the analysis of images that depict either of the moons and the Earth-Moon system, the Galilean moons, the Martian surface, a star or a star field. These objects are very small and appear as point like light sources that are distorted by the SRC's specific point spread function. This requires special care to be taken when the data is reduced.

## 2. Observations

Table 1 provides an overview of existing mutual event observations from the start of the Mars Express mission in 2003 until March 2018. For all available Earth-Moon system observations the Moon is taken as reference object as the Earth itself is overexposed. This is

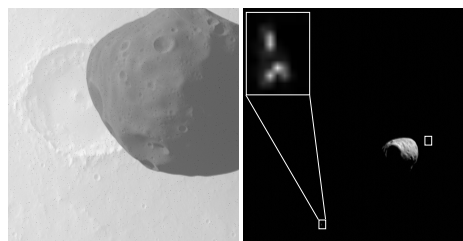


Figure 1: Left: Phobos above the Martian surface (SRC image HC266\_0004), right: Phobos and two stars (image HC563\_0005) [both ESA/DLR/FU Berlin].

Table 1: Number of images showing mutual events.

Martian moon	other object	# images
Phobos	star(s)	484
Phobos	Earth-Moon system	54
Phobos	Galilean moons	181
Phobos	Martian surface	27
Deimos	star(s)	91

a result of long exposure times necessary to observe Phobos.

## 3. Methods

The actual measurement is the determination of the image coordinates of the depicted bodies' center of figures (COFs). To support the measurements in given SRC images, synthetic images of Phobos and Deimos are computed. To this end, the observation geometry is simulated using the NAIF SPICE toolkit as well as shape models [10, 12], updated rotational models ([9]) and the parameterless Akimov disk function [4, 8], which describes the photometric behavior of the surface. The simulation is then used to detect the moon in one image (reference image) of each series. The part of the image containing only the detected moon

is used as a template for the matching process in all other images of this specific observation series. Since the COF location is known for the simulation, its location in the image can be easily determined once a good match between observation and simulation is achieved [13].

The SRC images are affected by a complex point spread function (PSF) owing to which stars appear as triangular objects with diffuse edges (see Fig. 1). A PSF provided by [1] is used to detect a star in the reference image. The section of the reference image containing the star is used as a template for the matching process in all other images. If several stars are contained in one image, each star is separately detected and a separate template is created, to take care of possible (albeit small) position-dependent distortions in the image. The stars are identified by means of the new Gaia catalogue [2].

Due to their small sizes and large distances to Mars Express, the Earth's moon and the Galilean satellites are comparable to point-like sources and the same approach for positional measurements as for stars is applied. In both series observing the Jupiter system all Galilean moons can be detected, i.e. none is occulted by Jupiter. However, in orbit 9463 Io and Europa are located close together making the determination of the separate positions difficult. The identification of the moons is supported by SPICE information.

For images of Phobos above the Martian surface the SRC viewing geometry and s/c position provide good information which Mars surface features (e.g. a crater) can be seen in the image. This provides the means to derive the position of the Martian COF in the image plane and hence the angular separation between Phobos and Mars.

## 4. Conclusions and Outlook

After successfully reducing mutual event observations involving either both Martian moons, Jupiter or Saturn [13], in this paper we describe the reduction of the remaining mutual events observations, which either show Phobos above the Martian surface or one of the moons with a point-like object in the background. The measured angular separation between the Martian moons and the respective background objects will be compared against existing orbit models, e.g. MAR097 [3] and NOE-4-2015-b. Previous results of [13] show a slightly better agreement between observations and the NOE-4-2015-b orbit model. The new observations are expected to complement the previous data set and yield improved ephemerides of the Martian satellites.

## Acknowledgements

This project is supported by the Deutsche Forschungsgemeinschaft (DFG), research grant number OB 124/14-1. The authors thank the HRSC Experiment teams for their successful planning and acquisition of data as well as for making processed data available to the HRSC team.

## References

- [1] Duxbury, T. et. al.: Mars Express Super Resolution Channel Image Restoration and Geometric Properties, HRSC Team Meeting 2011, Technical Note, 2011.
- [2] Gaia Collaboration, Brown, A. et.al.: Gaia Data Release 2. Summary of the contents and survey properties, accepted for A&A Special Issue on Gaia DR2, 2018.
- [3] Jacobson, R. A. and Lainey, V.: Martian satellite orbits and ephemerides, PSS, 102, pp. 35-44, 2014.
- [4] Longobardo, A. et. al.: Photometric behavior of spectral parameters in Vesta dark and bright regions as inferred by the Dawn VIR spectrometer, Icarus, 240, pp.20-35, 2014.
- [5] Oberst, J. et. al.: Astrometric observations of Phobos and Deimos with the SRC on Mars Express, A& A, 447, pp. 1145-1151, 2006.
- [6] Pasewaldt, A. et. al.: New astrometric observations of Deimos with the SRC on Mars Express, A&A, 545, A144, 2012.
- [7] Pasewaldt, A. et. al.: Astrometric observations of Phobos with the SRC on Mars Express: New data and comparison of different measurement techniques, A&A, 580, A28, 2016.
- [8] Shkuratov, Y. G. et. al.: Opposition Effect from Clementine Data and Mechanisms of Backscatter, Icarus, 141, pp. 132-155, 1999.
- [9] Stark, A. et. al.: Geodetic Framework for Martian Satellite Exploration I, European Planetary Science Congress 2017, 17-22 September 2017, Riga, Latvia.
- [10] Thomas, P. et. al.: Small Body Shape Models V2.1, NASA Planetary Data System, 173, <http://adsabs.harvard.edu/abs/2000PDSS...173.....T,2000>
- [11] Willner, K. et. al.: New astrometric observations of Phobos with the SRC on Mars Express, A& A, 488, pp. 361-364, 2008.
- [12] Willner, K.: Phobos' shape and topography models, PSS, 102, pp. 51-59, 2014.
- [13] Ziese, R. and Willner, K.: Mutual event observations of solar system objects by SRC on Mars Express, A&A, in press, 2018.

# DRAGON: the Deimos Reconnaissance And Geological Observation CubeSat

Erik Asphaug<sup>1</sup>, Jekan Thangavelautham<sup>2</sup>, James Uglietta<sup>2</sup>, Ravi Teja Nallapu<sup>2</sup>, Aman Chandra<sup>2</sup>, Leonard Vance<sup>2</sup>, Stephen Schwartz<sup>1</sup>. <sup>1</sup>Lunar and Planetary Laboratory, University of Arizona, Tucson AZ (asphaug@lpl.arizona.edu), <sup>2</sup>Space and Terrestrial Robotics Laboratory (SpaceTReX), Aerospace and Mechanical Engineering, University of Arizona, Tucson AZ

## Abstract

Phobos and Deimos, the small moons of Mars, are potentially key players in the human settlement of space. Whether that settlement ends up being primarily robotic or human, or robot-assisted and how, and what types of settlements are feasible and on what timescale, and how to begin, depend on variables that we are just beginning to find out.

Towards that goal, we propose the low-cost pathfinder mission DRAGON, the Deimos Reconnaissance And Geologic ObservatioN CubeSat, whose goal is to provide unique data about the most valuable surface locations on Deimos in preparation for the first soft landings there. This mission concept builds upon a two-year student-led effort, with enhancements aimed at obtaining unique, priority reconnaissance data of Martian moons Phobos and Deimos ahead of future landings.

## 1. Introduction: Phobos or Deimos?

The Martian moons have significant advantages compared to most asteroids when it comes to establishing a long term presence in deep space [1]. Deimos has two small regions at sub-Mars latitudes (60°N, 0°W; 51°S, 7°E) that offer constant line of sight to Earth and the Sun in summer and winter, respectively. Moreover, orbiting just outside Mars geosynchronous radius  $\sim 6R_{Mars}$ , Deimos maintains persistent line of sight with any location on the planet surface for as long as 60 hr on the equator.

Phobos orbits every 8 hr, thus has at most 4 hr persistent communication with a site on Mars. Moreover, Phobos orbit is so close that Mars spans 42.5° in Phobos' sky, meaning that the highest latitudes of Mars are obscured. Lastly, the propulsion requirements for matching orbits with Deimos are  $\sim 750$  m/s less than for Phobos.

Phobos has been the focus of multiple mission concepts [2, 3], including In-Situ Resource Utilization Missions [4]. While Phobos might hold answers to more profound science questions, and is therefore the more fruitful target in the near-term for science missions such as JAXA's MMX (Mars Moons eXploration) mission [2], Deimos appears to offer the better 'high ground' supporting long term human presence [1].

## 2. Mission Concept

CubeSats offer the opportunity to perform low-cost, focused science exploration, with rapid turn-around times between multiple missions. We propose development of a 12U, 24 kg interplanetary CubeSat called DRAGON that would perform reconnaissance of Deimos at altitudes of 5 km and less over a 2-year mission.

DRAGON is inspired by JPL's INSPIRE and MarCO CubeSats on the way to Mars. The CubeSats would be dropped-off on an Earth Escape trajectory to Mars much like the MarCO CubeSats (**Fig. 1**) or contain a propulsive ESPA stage that would put it on a flyby trajectory to Mars.

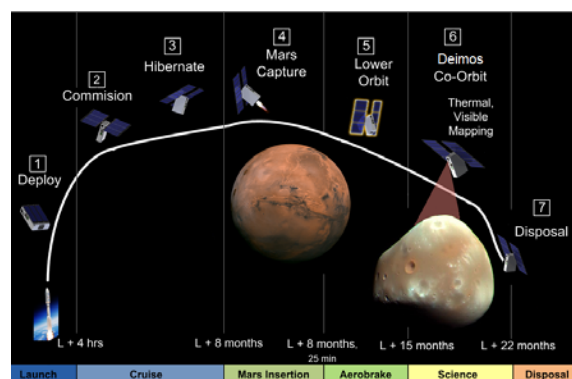


**Fig. 1.** DRAGON Concept of Operations.

The spacecraft upon reaching Mars may use on-board propulsion to achieve a highly elliptical capture orbit that is then regularized through multiple aero-drag maneuvers by passing through the Martian atmosphere. An alternative is a one-shot aero-capture maneuver that places the spacecraft in an elliptical co-orbit with Deimos.

### 3. Spacecraft

The CubeSat, a 12U, 24 kg spacecraft will be developed by Space Dynamics Laboratory (Utah State University). The CubeSat will be equipped with a pair of MMA eHawk+ solar panels providing ~40 watts at Mars and high-gain communications antenna with 40+ dBi gain enabling transmission of high-resolution images and short videos direct to earth. The spacecraft would contain JPL's Iris transceiver for communication and Doppler tracking through the DSN, an on-board high delta-v chemical propulsion system and rad-hardened electronics to withstand a multi-year mission in deep space.

### 4. Science Instruments

The instrument suite onboard DRAGON are tentatively as follows:

1. Telescopic color imager for highest resolution imaging from a sequence of slow flyovers.
2. Thermal imager for understanding the nature (e.g. particle size) of the upper regolith
3. Point-spectrometer for mineral characterization of selected regions
4. Wide angle b/w imager, for final images prior to the terminal impact.

### 5. Operations

The DRAGON mission is designed to make a first close-up assessment of these optimal sites on Deimos by making use of breakthroughs in CubeSat propulsion, instrumentation and communications technology to perform a sequence of slow flybys over 2 years followed by a terminal impact. Repeated close encounters with Deimos over a 2-year period will provide sufficient high-resolution images for meeting the mission reconnaissance goals. Spacecraft observations are focused on obtaining

data only from these northern and southern hemispheric 'sweet spots', with a goal of minimizing risk for future soft landings.

The proposed mission campaign has three phases:

1. **Close Flyovers.** At least 2 low-velocity (<100 m/s) flyovers, of each N and S target region  $100 \times 100 \text{ m}^2$ , from closest approach distance of <5 km
2. **Descent Imaging.** Take pictures of the predicted crash site, coverage over an area of  $3 \text{ m} \times 3 \text{ m}$ .
3. **Free Fall.** At a predicted time, the spacecraft fires a reverse thruster to cancel its free-fall velocity, resulting in it hovering above the surface for some minutes until it lands.

### 6. Mission Finale

The terminal impact will follow a retro-burn that will slow the spacecraft to a few m/s before making a surface impact. Due to Deimos' low gravity, the terminal impact is expected occur over a few minutes allowing for transmission of multiple high resolution images of candidate landing sites.

The highest resolution final images, at better than 1 cm/pixel, are the top level science goal. We do not expect survival of the spacecraft on the surface, although the wide angle camera can continue to transmit if the spacecraft does survive.

### Acknowledgements

We are grateful for the contributions of G. Dektor, N. Kenia, S. Ichikawa, A. Choudhari, and M. Martinez.

### References

- [1] Hopkins, J.B. and Pratt, W.D., Comparison of Deimos and Phobos as Destinations for Human Exploration and Identification of Preferred Landing Sites, SPACE 2011 Conference & Exposition, AIAA, 2011-7140 27 - 29
- [2] H. Miyamoto "Japanese mission of the two moons of Mars with sample return from Phobos," Mars Exploration Program Analysis Group, Pasadena, California, 2016.
- [3] P. Lee, et al., "Phobos And Deimos & Mars Environment (PADME)," LPSC Conference XLVI, 2015.
- [4] A.C. Muscatello et al., (2012) "Phobos and Deimos Sample Collection Missions for Science and ISRU," Lunar and Planetary Science Conference (LPSC) 2012, 4296.

# Equipotential surfaces and geodetic implications on formation of Martian moons

Xuanyu Hu (1), Jürgen Oberst (1,2) and Konrad Willner (2)

(1) Institute of Geodesy and Geoinformation Science, Technical University of Berlin. (2) Institute of Planetary Research, German Aerospace Center (DLR Berlin-Adlershof). (xuanyuhu@gmail.com)

## Abstract

We determine the *normal ellipsoids* for the Martian moons, Phobos and Deimos, that closely approximate the equipotential surfaces in the respective gravity fields. We compare the normal ellipsoids with the actual shapes of the moons and discuss the implications on their formation. In particular, we revisit and explore the plausibility that the moons were formed out of the debris disk around Mars by material accretion under self-gravity.

## 1. Introduction

The Martian moons, Phobos and Deimos, are in distinct, near-circular orbits around Mars [1]. Both are tidally locked and thus rotate synchronously in their respective orbits around Mars. There has been ongoing, vigorous discussion about the origins of the moons. They may have been extraneous objects captured by the martian gravitation during chance encounters [2]; alternatively, they may have accreted *in situ* out of debris disk after impacts or tidal break-ups of asteroids [3, 4], a process that might occur repeatedly [5]. Studying the origins and evolution of the moons could cast light on the formation of the entire Martian system or that of any planetary system in general.

## 2. Method for deriving normal ellipsoid

Phobos is subject to significant tidal forces comparable to gravitation and centrifugal forces in magnitude. Deimos' orbit is at a greater distance and not as strongly influenced by tidal forces as Phobos. We are interested in the equipotential surfaces of both irregular-shaped moons, where the gravity potential is constant. For instance,  $W = W_0$  where  $W_0$  corresponds to the average potential over the surface of

the body. The equipotential surface indicates an idealized, equilibrium form that may or may not be close to the actual shape of the body. Specifically, we derive an ellipsoidal approximation of the equipotential surface, defined as the “normal ellipsoid” of the object. We split the gravity potential into a regular, dominant component,  $U$ , arising from the ellipsoidicity (e.g., polar and equatorial flattenings) of the attracting body, and small higher frequency disturbances,  $\delta W$ , such as

$$W = U + \delta W. \quad (1)$$

Thus,  $U$  is attributed to the gravity potential of the normal ellipsoid.

For Phobos and Deimos whose shapes are moderately irregular (e.g., overall convex without global concavities), it is reasonable and practical to model their gravitational fields by ellipsoidal harmonic series which yield reliable performance close to the surface [6, 7]. We apply an iterative approach to search for the normal ellipsoid such that the following conditions are satisfied: (A)  $U = W_0$  and fully accounts for field variations up to degree two on the normal ellipsoid; (B)  $\delta W$  only appears from degree three or higher degrees [7].

## 3. Result

The method has been applied to deriving the normal ellipsoid of Phobos. Using the shape model presented in [8] and assuming homogeneous density for the body [9], the average gravity potential on the surface of Phobos is found as  $W_0 = 67.57 \text{ m}^2\text{s}^{-2}$ . The normal ellipsoid of Phobos has three semi-axes of 14.70, 10.58, and 8.94 km, thus notably elongated from its actual shape. The elongation of the normal ellipsoid occurs in the direction towards Mars (which lies along the  $x$  axis, see Fig. 1), evidently due to tidal effects. Meanwhile, the elongation concurs with a contraction of the normal ellipsoid along the transverse plane from the actual shape of Phobos (near  $x = 0$ , Fig. 1c). We

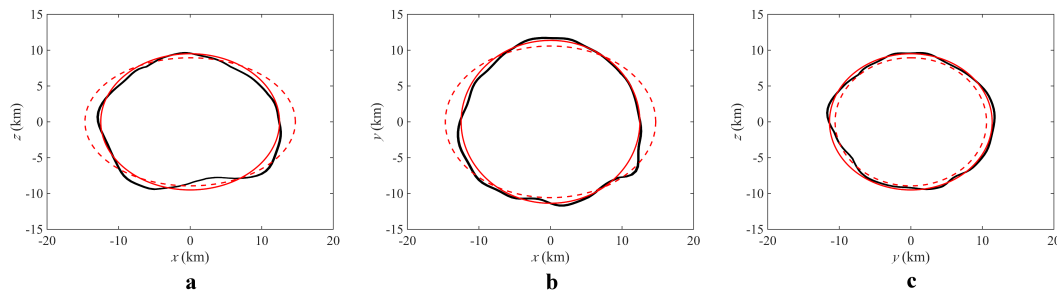


Figure 1: Projections of the normal ellipsoid in comparison with those of the actual shape of Phobos [8]. The shape of Phobos is indicated by the solid black lines. The normal ellipsoid is indicated by the red lines. The dashed and solid lines correspond to the tidally elongated and tide-free ellipsoids, respectively. This figure is adapted from Fig. 7 in [7].

also derived the normal ellipsoid of Phobos in a tide-free environment, with semi-axes of 12.49, 11.38, and 9.50 km, that corresponds to a slightly reduced surface potential of  $66.48 \text{ m}^2\text{s}^{-2}$ . The shape of Phobos undulates more evenly about its equilibrium figure in the absence of tidal effects (Fig. 1).

#### 4. Summary and outlook

That the current shape of Phobos differs notably from an equipotential surface corroborates that it is subject to tidal deformation in the future, the signs of which are perhaps already present [10, 11]. On the other hand, that Phobos would be close to equilibrium in an otherwise tide-free environment alludes to its formation dominated by gravitational aggregation [12], producing a porous rubble-piled structure with low bulk density [3, 4].

Work is being carried out to derive the normal ellipsoid of Deimos, which resides in a higher orbit of about 23500 km from (the center of) Mars and, thus, subject to less pronounced tidal effect.

#### References

- [1] Jacobson, R. A.: The orbits and masses of the Martian satellites and the libration of Phobos, *The Astronomical Journal*, 2010
- [2] Pollack, J. B., Veverka, J., Pang, K., et al.: Multicolor Observations of Phobos with the Viking lander cameras: evidence for a carbonaceous chondritic composition, *Science*, 199, pp. 66-69, 1978
- [3] Craddock, R. A.: Are Phobos and Deimos the result of a giant impact? *Icarus*, 211, pp. 1150-1161, 2011
- [4] Rosenblatt, P., Charnoz, S., Dunseath, K. M., et al.: Accretion of Phobos and Deimos in an extended debris disc stirred by transient moons, *Nature Geoscience*, 9, pp. 581-583, 2016
- [5] Hesselbrock A. J., and Minton, D. A.: An ongoing satellite-ring cycle of Mars and the origins of Phobos and Deimos, *Nature Geoscience*, 10, pp. 266-269, 2017
- [6] Garmier, R. and Barriot, J.-P.: Ellipsoidal harmonic expansions of the gravitational potential: theory and application, *Celestial Mechanics and Dynamical Astronomy*, 79, pp. 235-275, 2001
- [7] Hu, X.: Normal gravity fields and equipotential ellipsoids of small objects in the Solar System: a closed-form solution in ellipsoidal harmonics up to the second degree, *The Astrophysical Journal*, 850:107(19pp), 2017
- [8] Willner, K., Shi, X., and Oberst, J.: Phobos' shape and topography models, *Planetary and Space Science*, 102, pp. 51-59, 2014
- [9] Andert, T., Rosenblatt, P., Pätzold, M., et al.: Precise mass determination and the nature of Phobos, *Geophysical Research Letters*, 37, L09202, 2010
- [10] Shi, X., Oberst, J., Willner, K.: Mass wasting on Phobos triggered by an evolving tidal environment, *Geophysical Research Letters*, 43, pp. 12371-12379, 2016
- [11] Hurford, T. A., Asphaug, E., Spitale, J. N., et al.: Tidal disruption of Phobos as the cause of surface fractures, *Journal of Geophysical Research: Planets*, 121, pp. 1054-1065, 2016
- [12] Richardson, D. C., Leinhardt, Z. M., Melosh, H. J., et al.: Gravitational aggregates: evidence and evolution, in *Asteroids III*, 2002

# Spectral and Thermophysical characterization of a Phobos regolith simulant for MMX mission

A. Maturilli (1), H. Miyamoto (2), T. Niihara (2), M. Grott (1), J. Knollenberg (1), J. Helbert (1), N. Sakatani (3), K. Ogawa (4)

(1) Institute of Planetary Research, German Aerospace Center DLR, Rutherfordstr. 2, 12489 Berlin, Germany – [alessandro.maturilli@dlr.de](mailto:alessandro.maturilli@dlr.de)

(2) Dept. Systems Innovation, University of Tokyo, Tokyo 113-8656, Japan

(3) Institute of Space and Astronautical Science, Japan Aerospace Exploration Agency, 3-1-1 Yoshinodai, Sagami-hara, 252-5210, Japan

(4) Department of Planetology, Kobe University, 1-1 Rokkodaicho, Nada, Kobe, 657-8501 Hyogo, Japan

## Abstract

The two natural satellites of Mars, Phobos and Deimos are both important targets for scientific investigation. The JAXA mission Martian Moons eXplorer (MMX) is designed to explore Phobos and Deimos, with a launch date scheduled for 2024. The MMX spacecraft will observe both Martian moons and will land on one of them (Phobos, most likely), to collect a sample and bring it back to Earth.

The designs of both the landing and sampling devices depend largely on the surface properties of the target body and on how its surface is reacting to an external action in the low gravity conditions of the target. The Landing Operation Working Team (LOWT) of MMX started analyzing previous observations and theoretical/experimental considerations to better understand the nature of Phobos surface material, developing a Phobos regolith simulant material for the MMX mission [1].

At the Institute for Planetary Research of the German aerospace Center (DLR) in Berlin we performed a spectral and thermophysical characterization of the Phobos regolith simulant.

## 1. Composition of Phobos regolith

The composition of Phobos regolith still remains controversial despite decades of telescopic and remote based observations. Reflectance spectrum of Phobos is generally featureless and very dark, with at least two major spectral units identified (a red and a blue unit). Visible to near infrared spectroscopy study show that the moons' surfaces resemble D- or T-type asteroids or carbonaceous chondrite [2]. The

origin of the two Mars moons is still debated: current hypotheses are that Phobos and Deimos formed in situ in Mars orbit or by capture of asteroidal bodies originating outside the Mars system [2]. A recent study [1] showed that the spectral characteristics of both the blue and red units are not that different from each other, and their reflectance spectra are mostly similar to those of Tagish lake and CM2 chondrites.

## 2. Structure of Phobos regolith

Mechanical properties of the surface soil (bearing capacity, bulk frictional coefficient, and other parameters) are crucial parameters for designing a lander/sample collector, and also for a good scientific understanding of surface processes active on Phobos. The mechanical properties of Phobos regolith are poorly constrained because of the difficulty in estimating the particle sizes, particle size-distributions, the packing density of the regolith and other frictional parameters. Thermal inertia values indicate that the average particle diameter is expected to be <2mm in most regions. Earth-based radar observations of Phobos, as well as previous studies on the Moon and Itokawa particles, help better modelling of the Phobos surface properties. Accounting for these considerations, we assume that the regolith structure of Phobos has at least three layers; (1) a thin uppermost layer (<3cm in depth) of micron-scale dusts accumulated at extremely low density, (2) a 10cm- to 3m-depth regolith layer with particles accumulated at relatively higher porosity, and (3) a >10m-depth regolith layer with lower porosity.

### **3. Univ. of Tokyo (UT) Phobos simulant**

A Tagish Lake-based simulant (UTPS-TB) was produced by crushing and Mg-rich phyllosilicates (asbestos-free serpentine), Mg-rich olivine, Magnetite, Fe-Ca-Mg carbonates, Fe-Ni sulfides into very fine particles, and then mixed with carbon nanoparticles and polymer organic materials. The mixing happened as first under wet condition; the mixture was then successively completely dried to adapt the compressible strength to that of Tagish Lake.

### **4. Spectroscopic measurements at PSL of DLR in Berlin**

The Planetary Spectroscopy Laboratory (PSL) of DLR in Berlin is a spectroscopic facility providing bi-directional and hemispherical reflection, transmission and emission spectroscopy of target materials. Bi-directional reflectance of samples is measured with variable incidence and emission angles between 13° and 85°, for sample temperature 170K to room temperature, under vacuum conditions, covering the 0.2 to above 200 μm spectral ranges. Two integrating spheres allow measuring hemispherical reflectance of samples under purging in the entire PSL spectral range. An external emissivity chamber (working under vacuum) features high efficiency induction system heating the samples to temperatures from 320K up to 900K [3].

At PSL we measured the Phobos simulant material sieved in 3 different grain size ranges: 400-500 μm, 1.6-2 cm, 3.55-4 cm. For each size separate, emissivity was measured in vacuum for sample temperature 320K (50°C). Bi-directional reflectance was measured under several phase angles conditions for sample temperatures between 170K (-100°C) and room temperature in the whole UV to FIR spectral range [4]. Hemispherical reflectance was measured under purging conditions on the sample at room temperature in the whole UV to FIR spectral range.

### **5. Thermophysical properties of Phobos regolith simulant**

Regolith thermophysical properties play a major role in explaining the exchange of radiative energy between the asteroid and its environment. The

knowledge of these parameters is needed to calculate several parameters related to the surface and subsurface temperatures. We are going to measure some thermophysical properties of the Phobos regolith simulant in at least the 3 already cited grain size ranges. We use a Transient Hot Strip to measure the thermal conductivity while minimizing the contact resistance and sensor heat capacity during the measurements. The measurements taken following this method are calibrated against standard materials. The sample container is placed inside a thermal vacuum chamber; measurements can be performed at temperatures of -150°C to +50°C. Soil mechanical properties for the difference grain size fractions will be studied too, trying to get information on the cumulative (mass) size distributions of each fraction, sphericity, angularity, and grain porosity if possible. Compressive/crushing strength measurements of the porous materials could also be possible.

### **5. Conclusion**

Spectral and thermophysical properties of a Phobos regolith simulant soil (developed from the University of Tokyo) will be measured. This study non only will increase the knowledge needed for landing and sampling on Phobos surface (MMX) but will be useful for the JAXA Hayabusa2 mission to asteroid Ryugu, being the MMX soil simulant material now part of a suite of Ryugu simulant materials, whose spectral and thermophysical properties are going to be measured.

### **References**

- [1] Miyamoto, H., et al.: Phobos environment model and regolith simulant for MMX mission, 49th Lunar and Planetary Science Conference (Abstract. No. 1882), 19–23 March 2018, The Woodlands, Texas, 2018.
- [2] Fraeman, A. A., et al.: Spectral absorptions on Phobos and Deimos in the visible/near infrared wavelengths and their compositional constraints, *Icarus* 229, 196–205, 2014.
- [3] Maturilli A, et al.: The Planetary Spectroscopy Laboratory (PSL), European Planetary Science Congress, 16–21 September 2018, Berlin, Germany, 2018.
- [4] Maturilli A, Helbert J, St. John JM, Head III JW, Vaughan WM, D'Amore M, Gottschalk M, Ferrari S: Komatiites as Mercury surface analogues: Spectral measurements at PEL. *EPSL*, Vol. 398, pp. 58-65, 2014.

## Martian Moons eXploration (MMX) : an overview of its science

K. Kuramoto (1,2), Y. Kawakatsu (1), M. Fujimoto (1), J.-P. Bibring (3), H. Genda (4), T. Imamura (5), S. Kameda (6), D. Lawrence (7), K. Matsumoto (8), H. Miyamoto (5), T. Morota (9), H. Nagaoka (1), T. Nakamura (10), K. Ogawa (11), H. Otake (1), M. Ozaki (1), S. Sasaki (12), H. Senshu (13), S. Tachibana (5), N. Terada (10), T. Usui (4), K. Wada (13), S. Watanabe (9), and MMX study team

(1) Institute of Space and Astronautical Science, Japan Aero-space Exploration Agency (3-1-1 Yoshinodai, Chuo-ku, Sagami-hara, Kanagawa 252-5210, Japan), (2) Hokkaido University (Kita 10, Nishi 8, Kita-ku, Sapporo, Hokkaido 060-0810, Japan, keikei@ep.sci.hokudai.ac.jp), (3) IAS, Univ. Paris-Sud 11, (4) Tokyo Inst. Tech., (5) Univ. of Tokyo, (6) Rikkyo Univ., (7) APL, Johns Hopkins Univ. (8) NAOJ, (9) Nagoya Univ., (10) Tohoku Univ., (11) Kobe Univ., (12) Osaka Univ., (13) PERC, Chiba Inst. Tech.

### Abstract

Martian Moons eXploration (MMX) is a round trip mission to the Martian moons, under phase-A study in ISAS/JAXA to be launched in 2024. This paper describes conceptual study results about MMX science.

### Science goals and requirements

The MMX mission places two science goals; 1) To reveal the origin of the Mars' moons under debate between capture origin and giant impact origin, and then to make a progress in our understanding of planetary system formation and of primordial material transport around the border between the inner-and the outer parts of the early solar system, 2) To observe processes that have impact of the evolution of the Mars system from the new vantage point and to advance our understanding of Mars surface environmental transition.

The mission requirements extracted from the breakdown of science goals and objectives are summarized as follows: 1) Retrieval of Martian moon regolith samples and determination of the moons' origin from their laboratory analyses, 2) Close-up observations of independent proxies of the moons' origin, 3) Sample analyses and close-up observations to reveal the formation of moons' building materials and long term evolution of the moons, 4) Ibid to constrain the Mars system evolution and its elementary processes.

### Sample science concepts

MMX will carry out multi-samplings from Phobos which may have compositional diversity as inferred from the existence of two end members of representative reflectance spectra. Main reasons for taking Phobos rather than Deimos as the sampling target are abundant pre-existing data that help landing site selection and the expected higher concentration of younger impact ejecta from Mars in the surface sample.

Regolith samples more than 10 g enough for detailed analyses of Phobos-indigenous materials will be collected with characterization of sampling sites in relation to bedrocks and surrounding geologic features. Isotopic, elemental and mineralogical compositions of sample particles will be examined with chronological analysis, which reveals the origin and cosmochemical nature of Phobos. If Phobos-indigenous materials are carbonaceous chondritic as favored from the reflectance spectra, capture origin is concluded. In this case, those data also tell us the birthplace and migration of Phobos precursor until the capture event had happened. If indigenous materials mostly show igneous rock textures with composition as a mixture of the Martian mantle and an exotic body, giant impact origin is concluded. In this case, samples may also tell us information on the source region of the moon-forming giant impactor, the age and processes of the giant impact event, and the physico-chemical state of primordial Martian mantle. Survey and analyses (if available) of younger materials ejected from Mars would provide us information on the evolutionary history of Mars.

### Mission Instruments

For close-up observations of the Martian moons, TENG00 (Telescope camera) and OROCHI (Wide angle multi-band cameras), MacrOmega (Near IR spectrometer), MEGANE (Gamma-ray and neutron spectrometer), LIDAR (Light detection and ranging), CMDM (Circum-Martian dust monitor) and MSA (Mass spectrum analyzer) are specified as nominal science instruments. Some optional mission instruments are under discussion (rover, deployable cameras, and etc.). MacrOmega and MEGANE will be provided from CNES and NASA, respectively.

These instruments will complementarily reveal the global properties of Phobos and Deimos and search for proxies of the moons' origin, building materials and long-term evolution independently of sample analyses. For instance, high spatial resolution imaging by TENG00 will be used to search for young geologic structures on which fresh bedrock materials are exposed. Visible to near IR multispectral imaging for such structures by OROCHI and MacrOmega will constrain the mineralogical composition of bedrock with a particular focus on whether hydrous minerals exist or not, a possible proxy indicative of Phobos origin. Those instruments are also used for the landing site selection, sampling site characterization, geologic studies, and observation of Mars atmosphere.

MEGANE will also constrain averaged abundances of hydrogen and other elements such as Si, Fe, and O in surface layers across several tenths cm depth with a resolution of hemisphere-scale or better, which enables to cross-check the bedrock composition(s) estimated by sample analyses and multispectral imaging. The elemental abundance ratios such as Si/Fe are another useful proxy of satellite origin. MSA will attempt to detect ion particles originated from H<sub>2</sub>O possibly outgassing from the moon's interior as well as the sputtered ions including metallic elements from the satellite surface. If a significant flux of H<sub>2</sub>O-derived ion components is detected as expected for an ice-bearing Phobos, its cold origin, or capture origin is favored.

LIDAR measures the global topography of Phobos, which contributes to studies of geologic features such as grooves and craters and estimation of mass distribution inside Phobos in combination with gravity field analyses using orbital tracking and positioning data. CMDM monitors the dust particle flux around the moons, which provides basic data to understand the space weathering, gardening

processes on the moon's surface, and possible dust ring formation. This helps to understand the nature of returned sample grains and the long term evolution of the surface of the Martian moons.

## Mission Profile

The mission study proceeds targeting the launch in 2024. Five years round trip will be made by use of chemical propulsion system. The outward interplanetary cruise takes about 1 year by the most efficient Hohmann like transfer to arrive at Mars in 2025. MMX chooses 3 years' stay in view of more science data obtained and better condition for the landing operation. The homeward interplanetary cruise takes about 1 year as well and the spacecraft will return to the Earth in 2029.

After the Mars orbit insertion, MMX is injected into an orbit near the Phobos' orbit and approaches to Phobos by reducing the phase difference with Phobos. MMX is subsequently injected into a quasi-satellite orbit around Phobos to start its close-up observation. MMX will take successively lower quasi-satellite orbits with minimum altitude from the Phobos surface 20 km or below. From these orbits, global imaging of Mars atmosphere is also conducted.

Phobos' gravity is weak, but stronger than that of Itokawa and Ryugu, which causes differences in the approach and landing sequence from that of Hayabusa2. MMX adopts a ballistic descent to reach right above a landing site just before a final vertical descent. After the short period of hovering, the final descent is conducted by free-fall without a thruster jet to avoid sample contamination and whirling up of regolith particles.

The sampling operation time correlates with the rotation period of Phobos about 7 hours and 40 minutes; In the case without capability to hibernate in night time on the Phobos surface, the time duration of the surface stay is limited in 2.5 hours by taking 1 hour margin to the day time of Phobos. The time duration that can be allocated for the sampling operation is 1.5 hours. Taking also into account the communication delay, ~10 min is allowed for the decision of a sampling point based on the high-resolution surface image transferred to the Earth from the landing site.